# Anti-inflammatory Actions of Acanthoic Acid-Related Diterpenes Involve Activation of the PI3K p110γ/δ Subunits and Inhibition of NF-κB

Paqui G. Través,[1,6] María Pimentel-Santillana,[1,6] Daniel Rico,[2] Nuria Rodriguez,[3] Thomas Miethke,[3] Antonio Castrillo,[1] Emmanuel A. Theodorakis,[4] Paloma Martín-Sanz,[1] Michael A. Palladino,[5,*] and Lisardo Boscá[1,*]

[1]Instituto de Investigaciones Biomédicas Alberto Sols, Centro Mixto CSIC-UAM, Unidad Asociada Universidad de las Palmas de Gran Canaria, Arturo Duperier 4, 28029 Madrid, Spain
[2]Structural Biology and BioComputing Programme, National Cancer Research Center (CNIO), Melchor Fernández Almagro 3, 28029 Madrid, Spain
[3]Institut of Microbiology and Hygiene, Medical Faculty Mannheim, University of Heidelberg, Theodor-Kutzer-Ufer 1-3, 68167 Mannheim, Germany
[4]Department of Chemistry and Biochemistry, University of California, San Diego, 9500 Gilman Drive, La Jolla, CA 92093-0358, USA
[5]Sierra Mesa Technologies, 3357 Fortuna Ranch Road, Encinitas, CA 92024, USA
[6]Co-first author
*Correspondence: mapdino@aol.com (M.A.P.), lbosca@iib.uam.es (L.B.)
http://dx.doi.org/10.1016/j.chembiol.2014.06.005

## SUMMARY

The effect of acanthoic acid analogs on the response to proinflammatory challenge was investigated. Some pimarane diterpenes are known activators of the LXRαβ nuclear receptors, but we show here that they also exert a rapid, potent, and selective activation of the p110γ and p110δ subunits of PI3K. Combination of these effects results in an important attenuation of the global transcriptional response to LPS in macrophages. PI3K/Akt activation leads to inhibition of the LPS-dependent stimulation of IKK/NF-κB and p38 and ERK MAPKs. Macrophages from LXRαβ-deficient mice exhibited an inhibition of these pathways similar to the corresponding wild-type cells. Silencing or inhibition of p110γ/δ suppressed the effect of these diterpenes (DTPs) on IKK/NF-κB and MAPKs signaling. Taken together, these data show a multitarget anti-inflammatory mechanism by these DTPs including a selective activation of PI3K isoenzymes.

## INTRODUCTION

Macrophages are key players in the innate immune response (Gordon, 2007). During the inflammatory process, the early stages are dominated by macrophages displaying inflammatory and tissue-destructive activities followed by tissue repair (Gordon and Martinez, 2010; Mantovani et al., 2004). To carry out these functions, macrophages have membrane receptors, which recognize antigens (such as Toll-like receptor [TLR] ligands or pathogen-associated molecular patterns); cytokines; and chemokines, which trigger the specificity of the innate immune response (Garantziotis et al., 2008; Nathan and Ding, 2010; Pasare and Medzhitov, 2004). TLRs exert essential func-

tions in the activation of innate immunity as sensors of microbial infection (Garantziotis et al., 2008; Trinchieri and Sher, 2007), leading to the killing and clearance of pathogens. Signaling downstream from TLRs involves the recruitment of distinct Toll/interleukin-1 receptor (TIR)-domain-containing adaptor molecules including the myeloid differentiation factor 88 (MyD88) and the TIR-domain-containing adaptor-inducing interferon β (IFNβ) (TRIF) (Akira and Takeda, 2004; Jin and Lee, 2008; Kawai and Akira, 2011; Kumar et al., 2009; O'Neill and Bowie, 2007). Most TLRs signal through MyD88-dependent pathway, whereas TLR3, the receptor recognizing double-stranded RNA (dsRNA), is coupled to TRIF. TLR4, the receptor for lipopolysaccharide (LPS), is the only receptor that engages both MyD88- and TRIF-dependent pathways. MyD88- and TRIF-dependent pathways result in the activation of the transcription factor nuclear factor kappa B (NF-κB). TLRs also activate phosphatidylinositol 3-kinase (PI3K)/Akt pathway, which plays an important role in cell migration, phagocytosis, and apoptosis (Díaz-Guerra et al., 1999; Fukao and Koyasu, 2003; Katso et al., 2001; Troutman et al., 2012) and regulates MyD88- and TRIF-dependent events (Arbibe et al., 2000; Hazeki et al., 2007; Sarkar et al., 2004). PI3K converts phosphatidylinositol 4,5-bisphosphate (PIP$_2$) into *phosphatidylinositol (3,4,5)-trisphosphate,* which acts as second messenger to activate downstream protein kinases, including Akt (Franke et al., 1995; Guha and Mackman, 2002). Indeed, PI3K activation in macrophages contributes to the negative regulation of the NF-κB pathway, decreasing the inflammatory response (Aksoy et al., 2005, 2012; Chaurasia et al., 2010; Díaz-Guerra et al., 1999; Guha and Mackman, 2002; Medina et al., 2010; van Dop et al., 2010).

The ability of natural and chemically modified diterpenes (DTPs) and polyphenols to impair inflammatory responses has been evaluated in the past years (Bremner and Heinrich, 2002; de las Heras et al., 2003; Palladino et al., 2003). Most of the studies on terpenes have focused on NF-κB pathway as a common target in the action of these compounds, explaining their anti-inflammatory and immunomodulatory

Cell Press
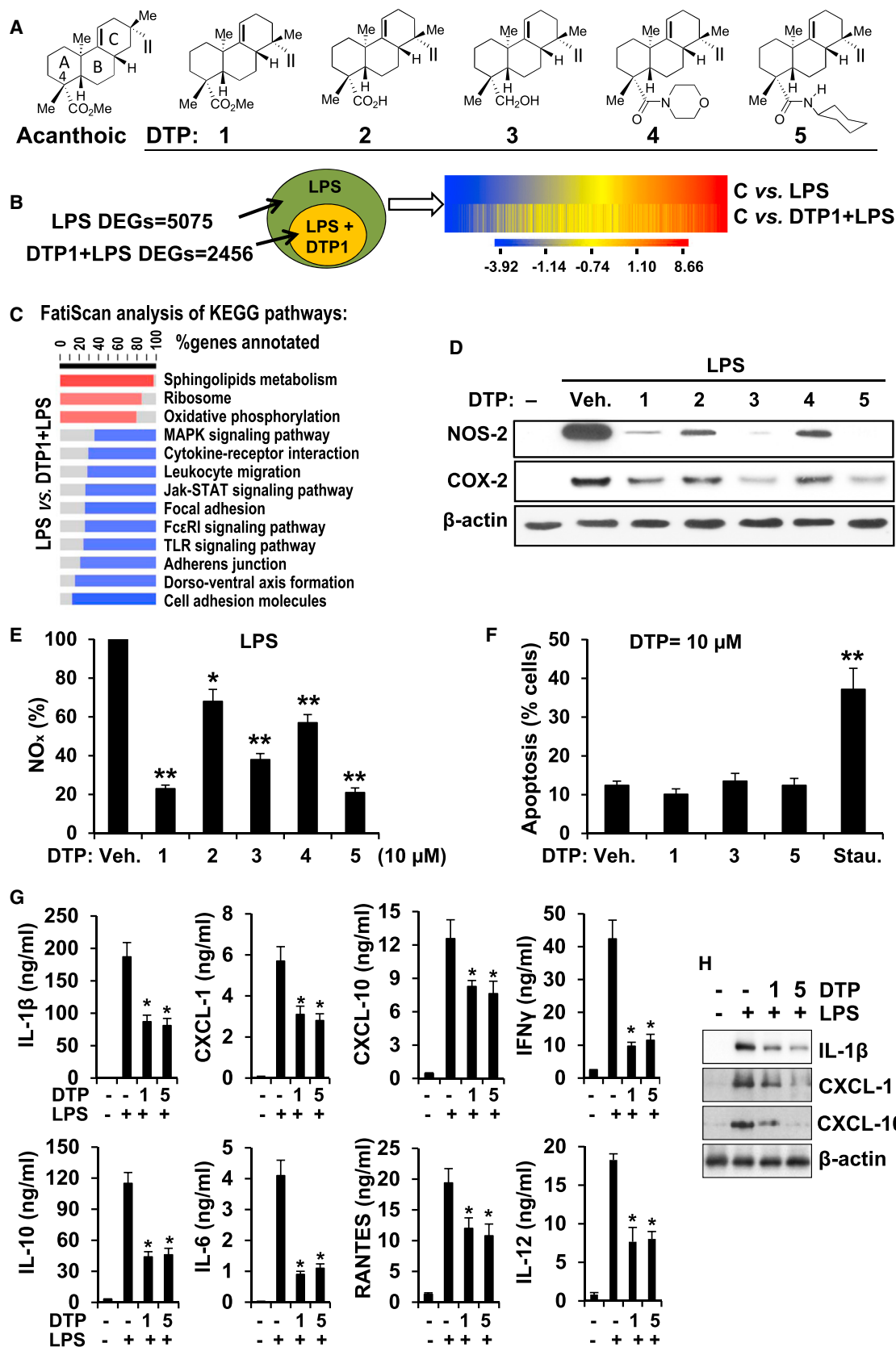


(legend on next page)

effects (Han et al., 2012; Nan et al., 2008). Indeed, several targets have been identified in this pathway, ranging from the inhibition of upstream kinases, NF-κB-inducing kinase and IκB kinase (IKK), and p65 phosphorylation, to the upregulation of the inhibitory proteins IκBα and Bcl-3. Some DTPs also activate nuclear receptors, such as liver X receptors (LXRs), contributing in this way to antagonize NF-κB activation by ligand-dependent transrepression (Castrillo et al., 2001a; de las Heras et al., 1999, 2003, 2007; Jayasuriya et al., 2005; Traves et al., 2007). Acanthoic acid exhibits in vivo anti-inflammatory activity inhibiting tumor necrosis factor α (TNF-α) production and exerting antifibrotic effects in models of experimental silicosis (Kang et al., 1996) and protective effects against fulminant hepatic failure in mice (Nan et al., 2008).

In this work, we have investigated the effect on macrophage activation and systemic inflammation of DTPs structurally related to acanthoic acid, with different substitutions at the carbon 4 position of ring A (Figure 1A). Previous studies showed that these DTPs activated LXRαβ and inhibited TNF-α release without noticeable effects on apoptosis in normal lymphoid cells (Chao et al., 2005; Traves et al., 2007). Our data extend these reports and show that DTPs exert a potent and selective activation of the p110γ and p110δ PI3K isoenzymes in macrophages. Moreover, the inhibition or silencing of these isoenzymes impairs the anti-inflammatory effects of DTPs on the early events of the IKK/NF-κB pathway and on the p38 and extracellular signal regulated-kinase (ERK) mitogen-activated protein kinase (MAPKs), even in the absence of LXRαβ. Oral or systemic administration of these DTPs confirmed the potential therapeutic role and safe profile of these molecules as anti-inflammatory drugs.

## RESULTS

### Acanthoic Acid-Related DTPs Inhibit the Expression of Genes Mediating Inflammation in Peritoneal Macrophages

The effect of DTP1, one of the five acanthoic acid C-4 derivatives assayed in this work (Figure 1A), on LPS transcriptional response in macrophages was analyzed. The profound impact of LPS on macrophage gene expression has been well characterized and even modeled by systems biology approaches (Tegnér et al., 2006). Accordingly, we identified a high number

of differentially expressed genes (DEGs; 5,075 genes, false discovery rate [FDR] ≤ 0.05) between control and LPS-stimulated cells (Figure 1B). Cotreatment with DTP1 and LPS resulted in ~50% reduction of DEGs (2,456 genes, using the same FDR threshold), indicating that DTP1 partially inactivates the transcription induced by LPS. Not only were fewer DEGs observed after DTP1 treatment but also attenuation of the LPS response was observed (Figure 1B, right). Functional enrichment of the Kyoto Encyclopedia of Genes and Genomes (KEGG) pathways analysis using FatiScan (Al-Shahrour et al., 2006) are shown in Figure 1C. Most of the pathways that were enriched in DTP1 downregulated genes were directly related with inflammation and immunity, such as the leukocyte migration, cytokine-receptor interaction, and TLR pathway. Given the key role of the TLR pathway in the macrophage-mediated inflammatory response, we characterized the genes belonging to this signaling cascade in more detail. The relative expression levels of the TLR pathway genes of macrophages treated with LPS and LPS + DTP1 are shown in Figure S1A (available online). Quantitative PCR (qPCR) analysis of selected genes of this pathway confirmed these trends and showed similar results between the DTP1 and DTP5 treatments (Figure S1B). Because DTP1 transrepresses a high number of inflammation-related genes, this effect was compared to that described for anti-inflammatory ligands that activated glucocorticoid receptor (GR), LXR, and peroxisome proliferator-activated receptor gamma (PPARγ) using published gene sets (Ogawa et al., 2005). This resulted in the target genes of the activated nuclear receptors (LXR, PPARγ, and GR) being significantly enriched in the panel of DTP1 downregulated genes (Figure S2); moreover, the DTP1 transrepression profile, in addition to overlapping with that of activated LXR (GW3965), also transrepressed LPS-induced genes that are LXR independent (those genes repressed exclusively by the GR ligand dexamethasone and the PPARγ ligand rosiglitazone, but not by GW3965). This implies that DTP1 represses the inflammatory response by LXR-dependent and -independent mechanisms.

We next designed a set of experiments to confirm the decreased transcriptional response to LPS induced by DTPs. Cells were incubated with DTPs and activated with LPS; then the expression of nitric oxide synthase-2 (NOS-2) and cyclooxygenase-2 (COX-2) (Figure 1D) and the accumulation of nitrate plus nitrite ($NO_x$) in the culture medium were measured

---

**Figure 1. Effect of Acanthoic Acid-Related DTPs on Inflammatory-Mediators Expression**

(A) Chemical structure of the five acanthoic acid C4 derivatives that were synthesized.

(B) Transcriptional response to LPS and DTP1 + LPS measured by gene expression microarrays. Peritoneal macrophages were pretreated with 10 μM DTP1 or the vehicle (DMSO) and then activated with 250 ng/ml of LPS for 4 hr. The number of significant DEGs (FDR ≤ 0.05) obtained after DTP1 + LPS is about half the number of DEGs after LPS + vehicle (left). The global fold changes (indicated in the heat map as log2) of LPS up- and downregulated genes were dramatically affected (right).

(C) Functional analysis of KEGG pathways using FatiScan resulted in 13 significantly enriched (FDR ≤ 0.05) pathways: three of them were enriched in genes upregulated (red) and the other ten were enriched in genes downregulated (blue) by DTP1.

(D–F) After 18 hr of incubation, the protein levels of NOS-2 and COX-2 (D) and the accumulation of $NO_x$ in the culture medium (E) were determined. Macrophages were incubated with staurosporine (200 ng/ml) or DTPs (10 μM) for 18 hr. Apoptosis was determined using flow cytometry using annexin-V labeling (F).

(G and H) Accumulation (after 18 hr) in the culture medium of IL-1β, CXCL-1 (KC), CXCL-10 (IP-10), IFN-γ, IL-6, RANTES, IL-10, and IL-12 (G). The intracellular levels of IL-1β, CXCL-1, and CXCL-10 were also determined at 18 hr (H).

Results show a representative blot out of three (D and H) and the mean ± SD (n = 4; E–G). *p < 0.05, **p < 0.005 versus the vehicle condition (E and F); *p < 0.05 versus the LPS condition (G).
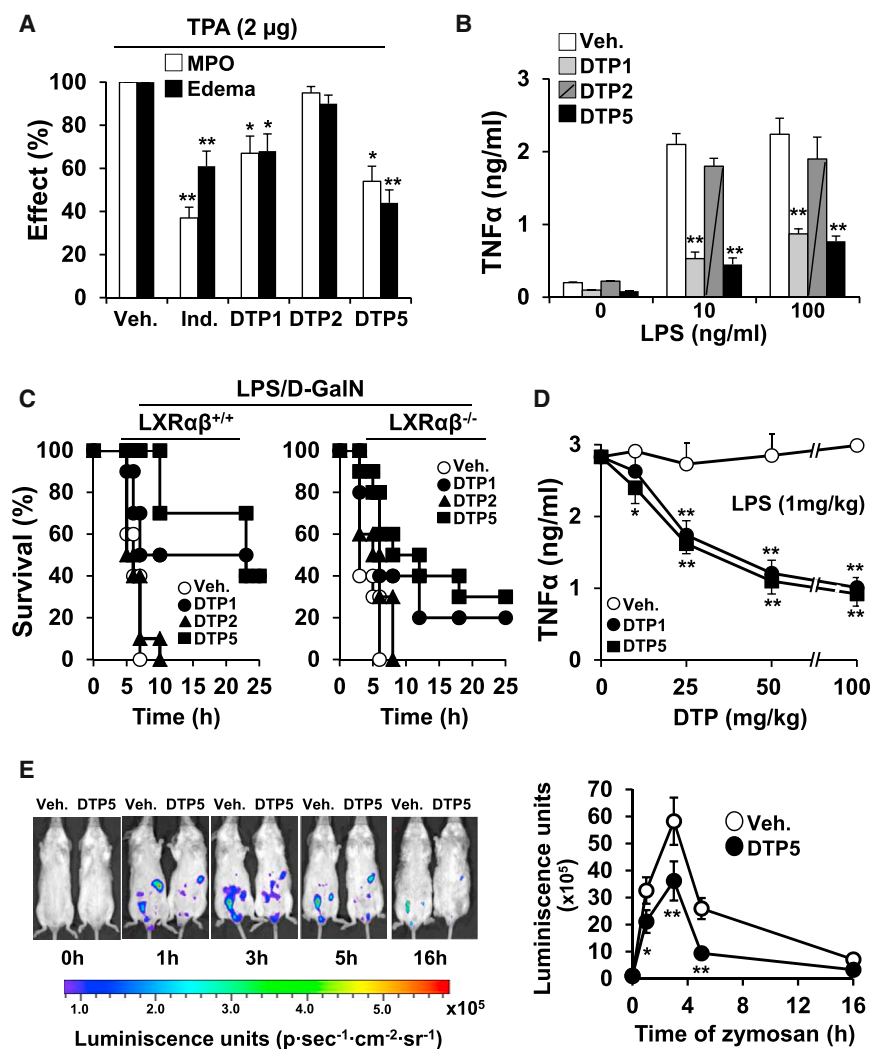
**Figure 2. DTP1 and DTP5 Inhibit TPA-Induced Ear Edema and Delay LPS/D-GalN Lethality**

(A) Male C57BL/6 mice received topically the indicated DTPs (0.5 μg in 20 μl DMSO) or indomethacin (0.5 μg in 20 μl) and TPA (2 μg in 20 μl). After 1 hr, animals were sacrificed and the MPO activity and the weight of identical sections of ear tissues were determined.

(B) Pooled whole-blood samples from C57BL/6J mice treated orally for 90 min with 25 mg/kg DTP1, DTP2, and DTP5 prepared in 40% Solutol HS15 (vehicle) were stimulated ex vivo with LPS at 10 ng/ml and 100 ng/ml for 4 hr, and the TNF-α levels were measured using ELISA.

(C) LXRαβ$^{+/+}$ and LXRαβ$^{−/−}$ mice were injected i.p. with 30 mg/kg body weight of the indicated DTPs and 1 hr later were i.p. conditioned with LPS/D-GalN. Results show the Kaplan-Meier representation of the survival time of the groups (n = 10).

(D) Similarly, LXRαβ$^{+/+}$ animals received i.p. the indicated concentrations of DTP1 and DTP5, followed 1 hr later by i.p. administration of LPS. The TNF-α plasma levels were measured at 1 hr after the LPS challenge.

(E) The in vivo effect of DTP5 (30 mg/kg; 1 hr prior to administration of 10 mg/kg zymosan) on MPO activity was measured in the whole animal by quantifying the bioluminescence after challenge with luminol (5 mg in 200 μl) using an IVIS-Lumina. Results show the mean ± SD (n = 5; A, B, D, and E). *p < 0.05, **p < 0.01 versus the corresponding control.

blood cells obtained from animals treated orally with DTP1 and DTP5 (not with DTP2) was decreased after LPS challenge (Figure 2B). The anti-inflammatory activity was also evaluated using the D-galactosamine (D-GalN)-sensitized LPS-dependent toxicity. As Figure 2C shows, only DTP1 and DTP5 exerted a significant protection against the lethality induced by LPS/D-GalN, both in LXRαβ$^{+/+}$ and LXRαβ$^{−/−}$ mice (p < 0.001 versus the treatment with DTP1 or DTP5 in both cases). In agreement with this, a dose-dependent inhibition of plasma TNF-α levels (1 hr after LPS) was observed when animals were injected intraperitoneally (i.p.) with DTPs and 30 min later were injected i.p. with LPS (1 mg/kg; Figure 2D). Also, inhibition of MPO activity was observed in vivo using bioluminescence recording after DTP5 (30 mg/kg) i.p. injection followed 1 hr later by zymosan (10 mg/kg) administration (Figure 2E).

(Figure 1E). DTP1, DTP3, and DTP5 exhibited an inhibition higher than 60% at 10 μM. To ensure that the inhibitory effects of these compounds were not due to cytotoxicity, we analyzed the percentage of apoptotic cells using staurosporine as positive control (Figure 1F). In agreement with the anti-inflammatory activity of DTP1 and DTP5, the accumulation in the culture medium of IL-1β, chemokine (C-X-C motif) ligand 1 (CXCL-1), CXCL-10, interferon γ (IFNγ), IL-6, chemokine ligand 5 (CCL5 or RANTES), IL-12, and the anti-inflammatory cytokine IL-10 were decreased in the presence of the DTPs (Figure 1G). The intracellular protein levels of some of these cytokines and chemokines were measured at 18 hr after LPS stimulation (Figure 1H).

### DTP1 and DTP5 Exert In Vivo Anti-inflammatory Activity
The anti-inflammatory action of DTP1, DTP2, and DTP5 was evaluated in a murine ear edema model. As Figure 2A shows, the myeloperoxidase (MPO) activity and edema due to infiltrated neutrophils after the topical application of tetradecanoylphorbol acetate (TPA) were significantly attenuated when animals received DTP1 and DTP5, but not after DTP2 (indomethacin was used as the control). In addition, TNF-α production by whole

### DTPs Inhibit the IKK/NF-κB and MAPKs Activation in Response to Different Proinflammatory Stimuli
DTP1, DTP3, and DTP5 activate LXRαβ, nuclear receptors that counteract NF-κB-dependent responses (Traves et al., 2007). Therefore, we designed a series of experiments to evaluate the anti-inflammatory effects mediated by DTPs independently of LXR activation. Figure 3A shows a potent inhibitory effect of DTP5 on NOS-2 and COX-2 protein levels regardless of the absence of LXRαβ. The dose-dependent effect of all DTPs on
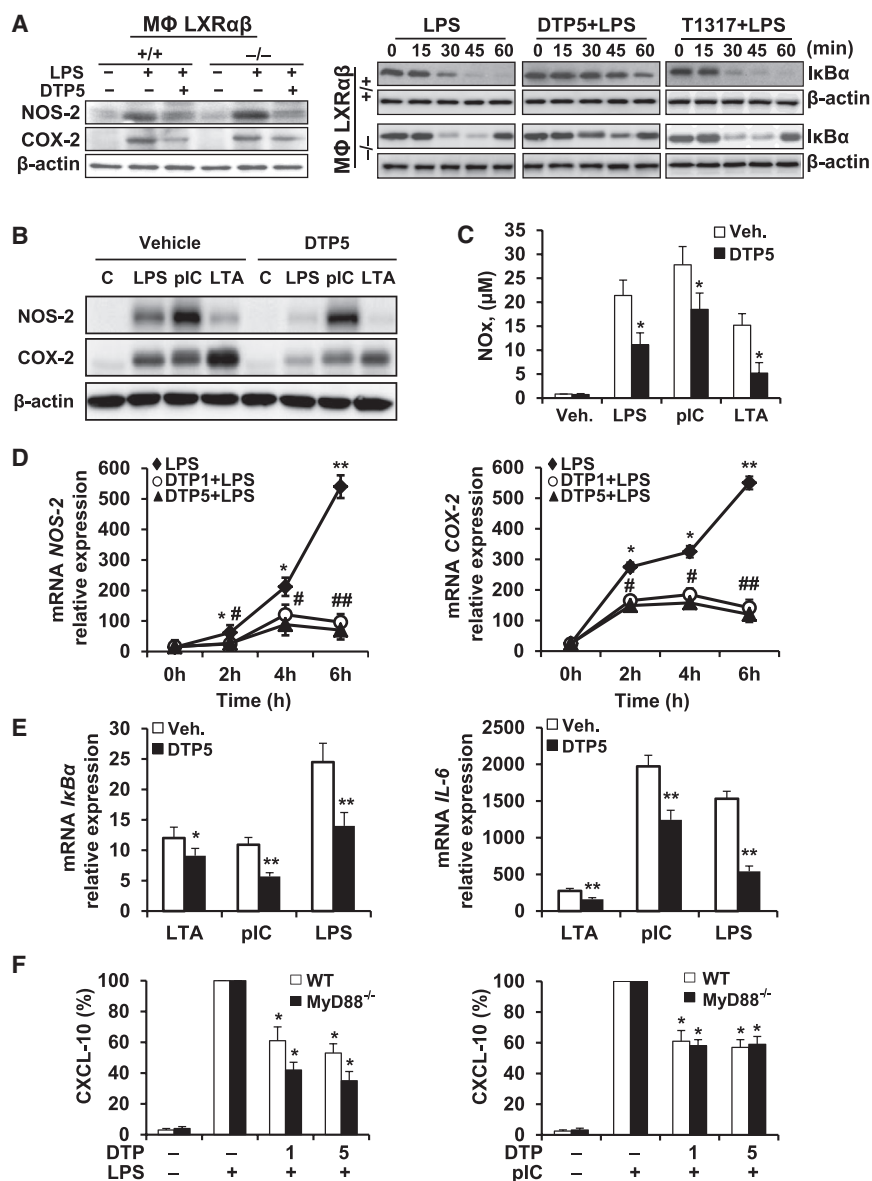
**Figure 3. The Anti-inflammatory Activity of DTPs in Macrophages Is Partially Independent of LXRαβ Nuclear Receptors and Independent of MyD88 Signaling**

(A) The levels of NOS-2 and COX-2 at 18 hr of treatment with LPS in the absence or presence of DTP5, and the time course of IκBα changes were determined in macrophages from LXRαβ^{+/+} and LXRαβ^{−/−} mice. T1317 (5 μM) was used as control for maximal activation of LXRαβ.

(B and C) The protein levels of NOS-2 and COX-2 (B), and the accumulation of $NO_x$ in the culture medium (C) were measured after challenge with LPS (250 ng/ml), LTA (5 μg/ml), or polyI:C (25 μg/ml) in cells pretreated with the vehicle or DTP5 (10 μM).

(D and E) The time course of the mRNA levels of *NOS-2* and *COX-2* (D), and the mRNA levels of *IκBα* and *IL-6* (E) at 4 hr after challenge with the indicated stimuli (E) were determined using q-PCR and normalized versus the housekeeping gene *36B4*.
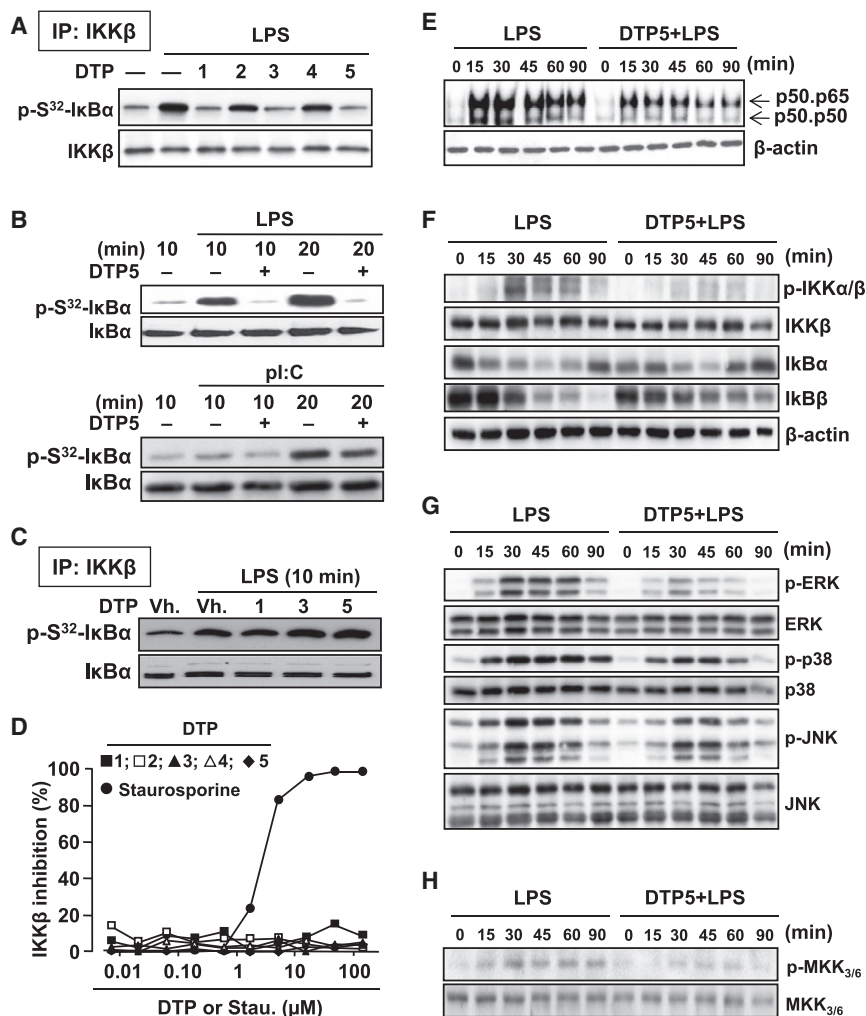
(F) The accumulation in the medium of CXCL-10 was measured in macrophages from WT or MyD88-deficient mice stimulated with LPS or polyI:C, as in (B), and expressed as a percentage versus the corresponding value with LPS or polyI:C alone (values were 14 and 10.6 ng/ml for WT and MyD88-KO mice treated with LPS, and 19.2 and 15.9 ng/ml for WT and MyD88-KO mice treated with polyI:C, respectively).

The blots show a representative experiment out of four (A and B), and the mean ± SD (n = 3; C–F). *p < 0.05, **p < 0.01 versus the corresponding condition in absence of DTP (C, E, and F); $^{+}$p < 0.05, **p < 0.01 versus the condition with the vehicle and $^{#}$p < 0.05, $^{##}$p < 0.01 versus the corresponding value without DTPs (D).

$NO_x$ accumulation after LPS treatment in LXRαβ^{+/+} and LXRαβ^{−/−} macrophages reflected a significant inhibition by the active DTPs (Figure S3A). The effect of DTP1 on the time course of NOS-2 and COX-2 expression was evaluated using LXRαβ^{−/−} macrophages (Figure S3B). Furthermore, DTP5 impaired IκBα degradation in LPS-treated cells, regardless the presence of LXRs. Nevertheless, the pharmacological activation of LXR with T1317 was not able to modify the IκBα degradation induced by LPS (Figure 3A), which agrees with previous work (Castrillo et al., 2003a). These results suggest that DTPs are also interfering with early signaling events after LPS challenge, independent of the LXRs activation. In addition to LPS, the response of macrophages to the TLR3 ligand polyriboinosinic:polyribocytidylic acid (polyI:C) and to the TLR2 ligand lipoteichoic acid (LTA) was analyzed. As Figure 3B shows, LPS, polyI:C, and LTA promoted the expression of *NOS-2* and *COX-2*, an effect

that was attenuated in the presence of DTP5. Moreover, the accumulation of $NO_x$ in the culture medium induced by these stimuli was also inhibited by DTP5 (Figure 3C). The time course of NOS-2 and COX-2 mRNA levels after LPS challenge showed an inhibitory effect by DTP1 and DTP5 (Figure 3D). Figure 3E shows the inhibitory effect of DTP5 on the *IκBα* and *IL-6* mRNA levels after the activation of TLR2, TLR3, and TLR4 with LTA, polyI:C, and LPS, respectively. When MyD88-deficient mice were used, DTP1 and DTP5 inhibited the accumulation of CXCL-10 in LPS and polyI:C-stimulated macrophages, regardless of the presence of MyD88 (Figure 3F). This suggests, together with the data from LTA treatment, that DTPs are effective in both the MyD88- and TRIF-dependent pathways.

Our data point to a possible effect of the DTPs at early signaling events after proinflammatory challenge; thus, to study the effect of these DTPs on IKK activation, we immunoprecipitated this enzyme from cells pretreated with the indicated DTPs (30 min) and then with LPS (10 min). The IKK activity was determined in vitro using purified IκBα as the substrate and measuring the phospho-Ser32-IκBα levels using specific

**A**

IP: IKKβ

LPS

DTP — — 1 2 3 4 5

p-S$^{32}$-IκBα

IKKβ

**B**

LPS

(min) 10 10 10 20 20
DTP5 − − + − +

p-S$^{32}$-IκBα
IκBα

pI:C

(min) 10 10 10 20 20
DTP5 − − + − +

p-S$^{32}$-IκBα
IκBα

**C**

IP: IKKβ

LPS (10 min)

DTP Vh. Vh. 1 3 5

p-S$^{32}$-IκBα
IκBα

**D**

DTP

■1; □2; ▲3; △4; ◆ 5
● Staurosporine

IKKβ inhibition (%)

DTP or Stau. (μM)

**E**

LPS       DTP5+LPS

0 15 30 45 60 90   0 15 30 45 60 90 (min)

← p50.p65
← p50.p50

β-actin

**F**

LPS       DTP5+LPS

0 15 30 45 60 90   0 15 30 45 60 90 (min)

p-IKKα/β
IKKβ
IκBα
IκBβ
β-actin

**G**

LPS       DTP5+LPS

0 15 30 45 60 90   0 15 30 45 60 90 (min)

p-ERK
ERK
p-p38
p38
p-JNK
JNK

**H**

LPS       DTP5+LPS

0 15 30 45 60 90   0 15 30 45 60 90 (min)

p-MKK$_{3/6}$
MKK$_{3/6}$

**Figure 4. Inhibition of NF-κB and MAPKs Pathways by Acanthoic Acid-Related DTPs**

(A) Macrophages were pretreated for 30 min with 10 μM of the indicated DTPs and then activated for 10 min with 250 ng/ml of LPS. The activity of IKK was assayed after immunoprecipitation (IP) of the enzyme and using purified IκBα as substrate and an Ab against p-Ser32-IκBα.

(B) The levels of p-Ser32-IκBα were determined using immunoblot in cells treated with 10 μM MG132 to inhibit proteasomal degradation.

(C and D) The direct effects of DTPs on purified IKKβ activity were determined after addition of 10 μM DTPs to the assay (C) and by homogeneous time-resolved fluorescence (HTRF) assays, using biotinylated IκBα (28–40 amino acids) as substrate and inhibition by staurosporine as a control (D).

(E–H) The effect of DTP5 on the LPS-activation of NF-κB was determined using EMSAs (E). The effect of DTP5 on the phosphorylation levels of IKK, IκBα, and IκBβ (F); ERK, p38, and JNK MAPKs (G); and the p38 upstream kinase MKK$_{3/6}$ (H) were determined using immunoblot.

Results show a representative experiment out of three.

dependent activation of the MAPKs ERK and p38 was inhibited by DTP5, whereas c-Jun N-terminal kinase (JNK) activation was less affected (Figure 4G). Consistent with these data, the phosphorylation of dual-specificity mitogen-activated protein kinase kinase 3 and 6 (MKK$_{3/6}$), an upstream kinase of p38 (Risco et al., 2012), was reduced in LPS-activated macrophages incubated with DTP5 (Figure 4H). In addition, activation with polyI:C or LTA of DTP5-pretreated macrophages showed a decreased IKK and p38 phosphorylation, but without noticeable effects on ERK and JNK phosphorylation (Figure 5). Taken together, these data pointed to early steps of IKK/NF-κB and MAPKs signaling as the main targets in the LXR-independent mechanism of action of DTP5.

**DTP1, DTP3, and DTP5 Activate the PI3K/Akt Pathway**

Previous reports indicate that the PI3K/Akt pathway plays a negative role on NF-κB activation in macrophages (Díaz-Guerra et al., 1999; Fukao and Koyasu, 2003). In view of our results presented here, we reasoned that this pathway was one likely candidate to mediate the effects of the DTPs. DTP1, DTP3, and DTP5, but not DTP2 and DTP4, promote the phosphorylation of Akt in Ser473, without altering Akt protein levels (Figure 6A). The time course of Akt phosphorylation by DTP5 is shown (Figure 6A, right). This S473-Akt phosphorylation was visualized using a confocal microscopy (Figure 6B), and the activation was also observed upon challenge with polyI:C or LTA (Figure 6C). In addition to Ser473-Akt, Thr308-Akt was also phosphorylated in response to DTP5 (Figure 6D). Furthermore, Akt was phosphorylated in vivo after the administration of DTP1, DTP3, and DTP5, but not with DTP2 and DTP4, in the TPA-induced ear edema

antibodies. Figure 4A shows a decreased activation of IKK in cells pretreated with DTP1, DTP3 and DTP5. Figure 4B shows the effect of DTP5 on the in vivo phosphorylation of IκBα in Ser32, analyzed after proteasome inhibition with MG132, in macrophages challenged with LPS or polyI:C. Furthermore, the in vitro addition of DTPs to immunoprecipitated IKK from LPS-treated cells did not affect the activity of this enzyme (Figure 4C). The direct effects of the DTPs on IKK were evaluated using recombinant IKKβ (that is constitutively active) and adding the DTPs to an in vitro homogeneous time-resolved fluorescence (HTRF) assay. As Figure 4D shows, the activity remained unaffected by the DTPs when assayed up to 100 μM. As expected, treatment with staurosporine, which was used as a positive control, inhibited IKK. The activation and translocation to the nucleus of NF-κB, evaluated using electrophoretic mobility shift assays (EMSAs), were significantly impaired when cells were incubated with DTP5 (Figure 4E) and DTP1 (not shown), which agrees with an LXR-independent effect. Figure 4F shows the time-dependent changes in IKK phosphorylation, which were less in the presence of DTP5, and the levels of IκBα and IκBβ, which showed a delayed degradation (for IκBβ), and a more rapid resynthesis (for IκBα). Under the same conditions, the LPS-
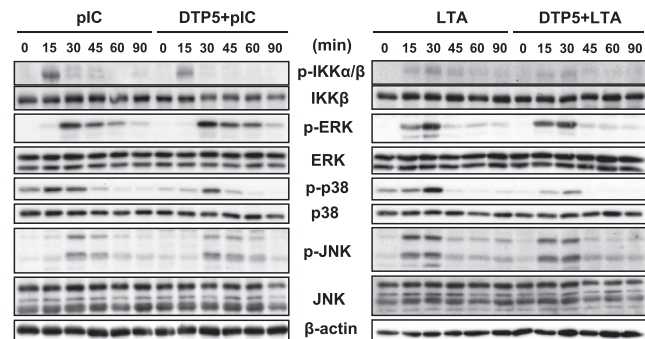
**Figure 5. Effect of DTP5 on IKK and MAPKs Activation in Macrophages Treated with polyI:C or LTA.**
Cells were treated as described in Figure 3B with polyI:C (25 μg/ml) or LTA (5 μg/ml), and extracts were prepared at the indicated times to determine IKK and MAPKs phosphorylation levels. Results show a representative blot out of four.

(Figure S4A) and in liver after i.p. administration of DTPs (Figure S4B). Akt phosphorylation was dependent on PI3K activation, as deduced by the determination of the PIP$_2$ phosphorylation in cell extracts immunoprecipitated with anti-p85 (Figure 6E). A positive control (50 nM insulin treatment) was included in the assay. Inhibition of PI3K with the broad inhibitor LY294002 suppressed Akt phosphorylation and PI3K activity. The effects of DTP5 on the inhibition of IKK, ERK, and p38 phosphorylation were attenuated when cells were treated with LY294002 (Figure 6F). Consistent results were obtained using LXR$\alpha\beta^{-/-}$ macrophages where the inhibition of Akt suppressed the effect of DTP5 decreasing NOS-2, COX-2, CXCL-1, and CXCL-10 levels (Figure S3C). Using NIH 3T3 cells transiently expressing a p110 wild-type (WT) or p110 kinase-deficient (KD) construct (Díaz-Guerra et al., 1999), the absence of p110 activity significantly decreased the DTP5-dependent phosphorylation of Akt (Figure 6G). LY294002 has been successfully used to clarify the physiological roles of PI3K; however, this compound is an effective inhibitor of all PI3K isoforms and of casein kinase 2 (Searl and Silinsky, 2005). To gain insights into the specificity of PI3K activation by DTPs, we used highly selective p110 isoenzyme inhibitors. The inhibition of p110$\gamma$ and p110$\delta$, and to a lesser extent of p110$\beta$, resulted in the suppression of the phosphorylation of Akt in response to DTP1 (Figure 7A). Indeed, the effect of DTP1 on IKK inhibition was reverted in the presence of the p110$\delta$ inhibitor, and more efficiently after dual inhibition of p110$\delta$ and p110$\gamma$ (Figure 7B). Because pharmacological studies always face the problem of specificity, we performed gene silencing with small interfering RNAs (siRNAs) specific for PI3K catalytic subunits (p110$\alpha$, p110$\beta$, p110$\delta$, and p110$\gamma$). The qPCR revealed significant knockdown of $p110\alpha$, $p110\beta$, $p110\gamma$, and $p110\delta$ expression using selective siRNAs (Figure S4C). In accordance with the pharmacological inhibitors, the levels of p-Akt increased by the action of DTP1 when the cells expressed p110$\gamma$ or p110$\delta$ (Figure S4D). Moreover, the ability of DTPs to directly activate PI3K was assayed after in vitro expression/translation of p110$\alpha$ (as a negative control) and p110$\delta$, and as Figure S4E shows, DTP5 enhanced the phosphorylation of PIP$_2$ only in the presence of p110$\delta$. In addition, using confocal microscopy and GFP-tagged Akt pleckstrin homology domain

(GFP-AktPH) as a molecular propidium iodide (PI)-sensor, we show that DTP1 promoted an increase in the fluorescence at the time that the probe aggregated in the perimembrane domain, suggesting a rapid and direct action of this DTP on PI3K activity (Figure S4F).

## DISCUSSION

Few studies have evaluated and molecularly characterized the anti-inflammatory effects of acanthoic acid, first isolated from the root bark of *Acanthopanax koreanum* Nakai, which has been used in traditional Korean medicine for the treatment of rheumatism and other chronic inflammatory diseases (Kang et al., 1996; Kim et al., 2004; Park et al., 2004), and now identified in other plants, including a bush native to California, *Coleonema puchellum*. Previous work using a series of synthetic analogs of this molecule identified the main structural motifs essential for their anti-inflammatory properties (Kang et al., 1996; Kim et al., 2004). As we described previously, some of these DTPs are potent activators of LXR$\alpha\beta$, which might explain in part their anti-inflammatory effects (Traves et al., 2007); however, these DTPs retain part of their anti-inflammatory activity when assayed in LXR$\alpha\beta^{-/-}$ mice. We found that the chemical modifications introduced in the DTPs, mainly positional modifications of the R-group at C4 of ring A, render molecules that have different quantitative effects on the expression of typical proinflammatory genes. Most of the studies in this report have been performed using DTP1 and DTP5 because these molecules exhibited greater effects in models of inflammation (effects persistent even in the absence of LXR$\alpha\beta$) that were chemically more stable than the other potent derivative, DTP3.

Our data show that DTPs negatively regulate inflammatory responses triggered by different TLRs, both in vitro and in vivo, decreasing the expression of cytokines, chemokines, and proinflammatory mediators. These DTPs significantly inhibit the IKK/NF-$\kappa$B pathway and the ERK/p38 MAPKs activated in response to LPS. These results are consistent with previous studies in which DTPs with kaurene structure, in addition to the NF-$\kappa$B pathway, also inhibited these MAPKs (Castrillo et al., 2001a). LPS activates TLR4, which is the only receptor able to signal through both MyD88-dependent and TRIF-dependent pathways (Aksoy et al., 2005; Gordon, 2007; Jin and Lee, 2008; O'Neill and Bowie, 2007). Similar results were obtained when macrophages were activated with TLR2 (MyD88-dependent) or TLR3 (TRIF-dependent) ligands. Interestingly, the absence of MyD88 (using CXCL-10 as the expression target) did not affect the inhibitory actions of DTPs upon challenge with LPS or polyI:C. All together, these data suggest the presence of a shared target for DTPs, common to the different signaling pathways analyzed but independent of MyD88 or TRIF. Moreover, these inhibitory effects persisted when the compounds were assayed in macrophages from LXR$\alpha\beta^{-/-}$ mice, pointing to an upstream nuclear receptor-independent mechanism. In this regard, the EMSAs demonstrated that DTPs reduced NF-$\kappa$B translocation to the nucleus in addition to the transrepression effects described for the LXRs inhibition of NF-$\kappa$B activity (Castrillo and Tontonoz, 2004; Traves et al., 2007). In a previous work, the action of these DTPs was assayed in LXR$\alpha\beta$ WT and KO mice after 24–48 hr of treatment with the DTPs (Traves et al., 2007); however, because LXR-deficient
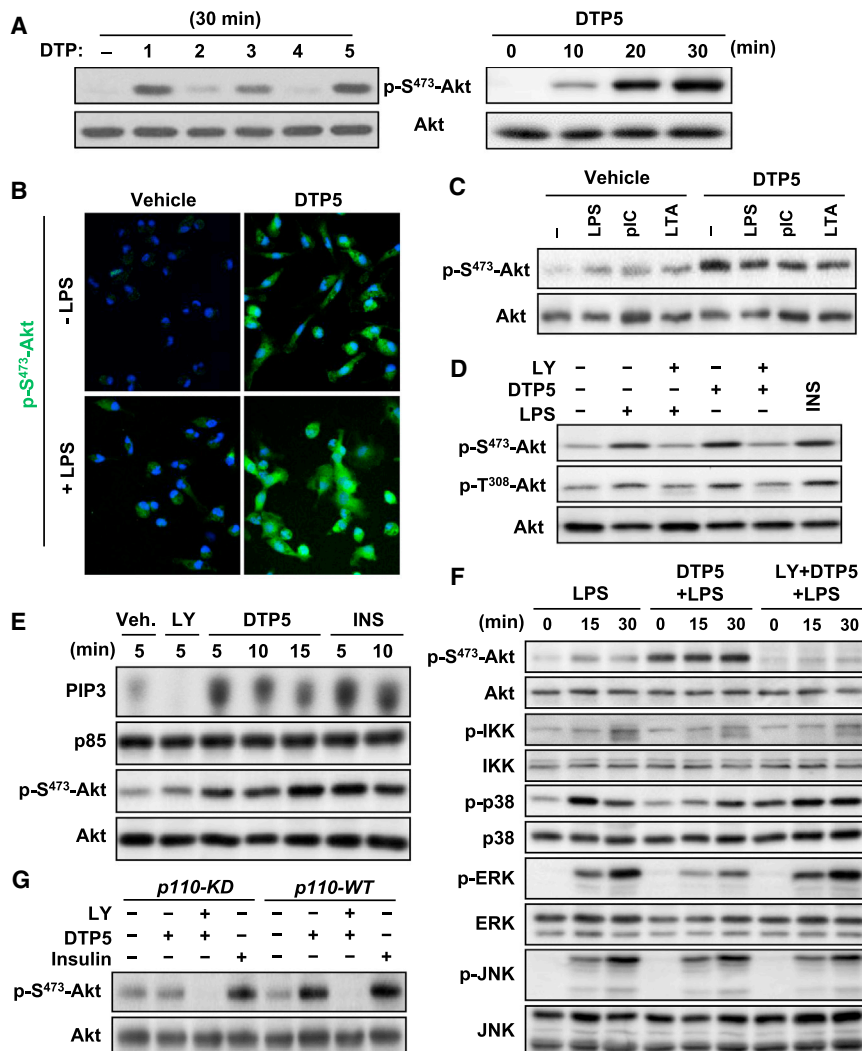
Figure 6. DTP1, DTP3, and DTP5 Activate the PI3K/Akt Pathway in Peritoneal Macrophages

(A) Cells were treated with the indicated DTPs (10 μM) for 30 min, and the levels of p-Ser473-Akt were determined (left). The time course of Ser473-Akt phosphorylation induced by DTP5 was analyzed (right).

(B) Visualization of p-Ser473-Akt (green) using a confocal microscopy. Nuclei were stained with DAPI (blue).

(C) Macrophages treated with the vehicle or DTP5 for 30 min were activated as in Figure 3B with LPS, polyI:C, or LTA (30 min), and the levels of p-Ser473-Akt were determined.

(D) The p-Thr308-Akt and p-Ser473-Akt were determined in cells incubated with LPS (250 ng/ml), DTP5 (10 μM), and LY294002 (10 μM); insulin (50 nM) was used as positive control. Cells incubated with DTP5 (10 μM), LY294002 (10 μM), and insulin (50 nM) for the indicated times were homogenized and immunoprecipitated with anti-p85 Ab.

(E) PIP2-kinase activity was determined in vitro and visualized using thin-layer chromatography. Samples of the extracts were used to determine p85 and p-Ser473-Akt/Akt levels.

(F) Effect of LY294002 on the time course of Akt, IKK, and MAPKs phosphorylation in macrophages treated with DTP5 and LPS.

(G) NIH 3T3 cells were transfected with a p110 kinase-deficient (KD) or wild-type plasmids, and the effect on p-Ser473-Akt levels was determined after incubation with LY294002 and DTP5. Insulin was used as a positive control.
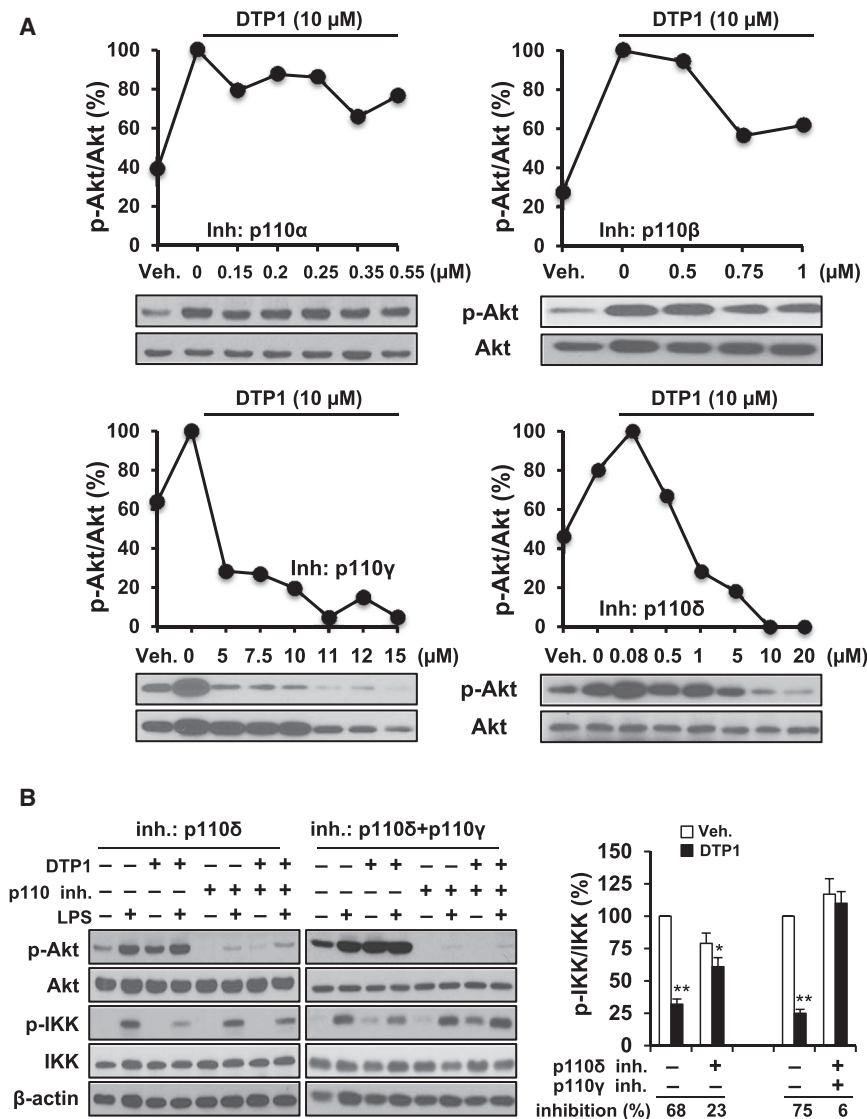
Results show a representative experiment out of three.

mice lack these proteins in all tissues and immunological alterations have been described (A-Gonzalez et al., 2013), we preferred to use WT animals and to evaluate the effects of DTPs for the short times analyzed in the present report. Studies in vivo with DTP1 and DTP5 showed a significant anti-inflammatory action in all the models assayed. The synthesis of TNF-α by whole blood collected from animals treated orally with these DTPs was inhibited; systemic i.p. administration significantly delayed the rate of animal death in a model of LPS/D-GalN-induced hepatotoxicity (even in the absence of LXRαβ), decreased the LPS-induced TNF-α plasma levels, and reduced the zymosan-induced peritoneal inflammation; and finally, the development of TPA-induced edema was also prevented to levels similar to those elicited by indomethacin.

When the inhibition of the NF-κB early signaling was investigated, we were unable to observe a direct effect of the DTPs on the activity of the IKK complex despite IKKβ phosphorylation being abrogated. Various reports show that PI3K contributes to the fine-tuning of the initial phases of the innate immune response to diverse microbial pathogens (Fukao and Koyasu, 2003; Hazeki et al., 2007; Ruse and Knaus, 2006). In dendritic cells and macrophages, the activation of PI3K/Akt was found to limit LPS-induced production of cytokines and chemokines and the expression of NOS-2 through both MyD88-dependent and -independent pathways (Aksoy et al., 2005). In this study, we have shown that DTP1, DTP3, and DTP5 induce a persistent Akt phosphorylation in vivo (ear edema and liver) and ex vivo (macrophages) at the two major sites, Thr308 and Ser473. We confirmed that this Akt activation was dependent on PI3K activity as far as it was suppressed by PI3K inhibitors. Furthermore, the phosphorylation of Akt in Ser473 was blocked by the expression of a kinase-deficient isoform of p110. In the same way, the involvement of the DTP-dependent activation of PI3K/Akt in the negative regulation of LPS-induced IKK, p38, and ERK phosphorylation was confirmed by the suppression of the DTPs effects after full PI3K inhibition (LY294002) or using selective p110γ/δ inhibitors and siRNAs. Taken together, these data contribute to a better understanding of the mechanisms of action of these DTPs in innate immunity. Finally, the dual action of DTP1, DTP3, and DTP5 on the PI3K/Akt/MAPK/NF-κB axis, on the one hand, and the selective activation of LXR, on the other, offers the possibility of modifying key cellular responses involved in many physiopathological processes in which macrophages play an active role in the onset of the disease, including inflammatory diseases, diabetes, and perhaps cancer.

**Figure 7. DTPs Induce p110γ/δ-Mediated Activation of Akt in Peritoneal Macrophages**

(A) Peritoneal macrophages were treated for 1 hr with increasing concentrations of highly selective inhibitors for the different p110 isoforms of the PI3K complex and then treated with DTP1 (10 μM; 30 min). The levels of p-Ser473-Akt were determined using immunoblot and expressed as a percentage versus the vehicle condition.

(B) Cells were incubated with p110γ (5 μM) and p110δ (1 μM) inhibitors for 60 min and then stimulated with DTP1 (10 μM; 30 min) and/or LPS (250 ng/ml; 30 min), as indicated. The effect of DTP1 on the phosphorylation levels of IKK after p110δ or after dual inhibition of p110γ/δ was determined using western blot. The band intensity ratio pIKK/IKK was expressed as a percentage versus the LPS condition in the absence of inhibitors and DTP. The relative inhibitory effect of DTP1 was calculated for each condition.

Results show one representative blot out of three (A and B) and the mean ± SD (n = 3) of the indicated band ratios (B, left). *p < 0.05; **p < 0.01 versus the corresponding condition in absence of DTP1.

Antibodies were from Santa Cruz Biotech, Cell Signaling, Abcam, PeproTech, Sigma-Aldrich, Millipore, and R&D Systems. Specific TLRs ligands (LPS from *Escherichia coli*, LTA, and polyI:C) were from Invivogen. Inhibitors LY294002, MG-132, PI3Kα inhibitor VIII, PI3Kβ inhibitor VI, and PI3Kγ inhibitor were purchased from Calbiochem. The PI3Kδ (CAL-101) inhibitor was from Selleck Chemicals. Electrophoresis and protein reagents were from Bio-Rad. Tissue culture dishes were from Falcon, and culture media and fetal calf serum (FCS) were from GIBCO (Life Technologies) and Sigma.

### Animals

Male mice were housed and bred in our pathogen-free facility and were maintained on standard chow under pathogen-free conditions. BALB/c were from Charles River Laboratories. LXRαβ$^{+/+}$ and LXRαβ$^{-/-}$ mice (mixed Sv129/C57BL/6 background) were obtained as previously described (Traves et al., 2007). MyD88$^{+/+}$ (WT) and MyD88$^{-/-}$ (KO) were obtained from a collaboration with Dr. T. Miethke (Institute for Medical Microbiology Immunology and Hygiene, Technical University of Munich). The study was conducted following the guidelines of the Spanish Animal Care and Use Committee, according to the guidelines for ethical care of experimental animals of the European Union (2010/63/EU).

### Peritoneal Macrophage Isolation

Animals were used at ages 8–12 weeks, as indicated in the online Supplemental Information.

### Cell Death Detection

Cells were collected and washed in cold PBS. After centrifugation for 5 min at 4°C and 1,000 × g, cells were resuspended in annexin V binding buffer (10 mM HEPES; pH 7.4, 140 mM NaCl, 2.5 mM CaCl$_2$) and labeled with annexin V–FITC (BD/PharMingen) and/or propidium iodide (PI; 100 μg/ml) for 15 min at room temperature (RT) in the dark, following a previous protocol (Hortelano et al., 2003). Analysis was carried out using a FC 500 BD FACScan flow cytometer.

## SIGNIFICANCE

**Our results demonstrate that these DTPs negatively regulate IKK/NF-κB and MAPKs (p38 and ERK) pathways by increasing p110γ/δ activity and, consequently, Akt phosphorylation. The ability of our compounds to selectively activate some isoforms of PI3K opens new prospects in the clinical development of anti-inflammatory molecules and points to the use of these acanthoic acid-related DTPs as anti-inflammatory and possibly anticancer drugs with potential therapeutic activity in inflammatory pathologies targeting simultaneously the PI3K/Akt, LXRαβ, and NF-κB pathways.**

## EXPERIMENTAL PROCEDURES

### Chemicals

Reagents were obtained from Sigma-Aldrich, Roche, Amersham-GE Healthcare, Merck, Bio-Rad, R&D Systems, and Promega. DTPs were synthesized by Prof. E. Theodorakis (University of California, San Diego) and were dissolved in DMSO before being used in cell culture (Ling et al., 2000, 2001).

### Determination of NO Synthesis
NO release was measured as the accumulation of nitrite and nitrate in the incubation medium (phenol-red free). Nitrate was reduced to nitrite with nitrate reductase and was determined spectrophotometrically with Griess reagent; the absorbance at 548 nm was compared with a $NaNO_2$ standard.

### Cytokine and Chemokine Assays
Cytokines production by cultured macrophages and its accumulation in the incubation medium were quantified using ELISA kits from PeproTech according to the manufacturer's instructions. Serum TNF-$\alpha$ was measured using Cytoset ELISA kits (Biosource International). Levels of CXCL-1 and CXCL-10 were measured using ELISA kits from R&D Systems according to the supplier's instructions.

### Quantitative PCR
We used 1 $\mu$g of total RNA, extracted with TRI Reagent (Ambion, Life Technologies) according to the manufacturer's instructions and processed as indicated in the online Supplemental Information.

### Preparation of Total Protein Cell Extracts
Cells were homogenized in a buffer containing 10 mM Tris-HCl (pH 7.5), 1 mM $MgCl_2$, 1 mM EGTA, 10% glycerol, 0.5% CHAPS, 1 mM $\beta$-mercaptoethanol, 0.1 mM phenylmethanesulfonylfluoride (PMSF), and a protease and phosphatase inhibitor cocktail (Sigma-Aldrich). The extracts were vortexed for 30 min at 4°C, and after centrifuging for 15 min at 13,000 × $g$, the supernatants were stored at −20°C. Protein levels were determined using the Bio-Rad reagent.

### Preparation of Cytosolic and Nuclear Extracts
Cells were collected into ice-cold PBS, resuspended in 200 $\mu$l of cytosolic buffer (10 mM HEPES; pH 8, 1 mM EDTA, 1 mM EGTA, 10 mM KCl, and 0.5% Nonidet P-40) and left to swell on ice for 15 min. The tubes were gently vortexed for 30 s, and the nuclei were collected using centrifugation at 13,000 × $g$ for 10 min (Castrillo et al., 2001a, 2003b). The supernatants were stored at −20°C (cytosolic extracts); the pellets were resuspended in 50 $\mu$l of nuclear buffer (20 mM HEPES; pH 8; 0.4 M NaCl, 1 mM EDTA, 1 mM EGTA, and 20% glycerol) and gently shaken for 30 min at 4°C. Nuclear protein extracts were obtained using centrifugation at 13,000 × $g$ for 10 min, and the supernatants were transferred to a fresh tube and stored at −80°C. Protein content was assayed using the Bio-Rad protein reagent. All cell fractionation steps were carried out at 4°C. All buffers contained protease and phosphatase-inhibitor cocktail (Sigma-Aldrich) (Prieto et al., 2010).

### Characterization of Proteins Using Immunoblot
Protein extracts were boiled in loading buffer (250 mM Tris-HCl; pH 6.8, 2% SDS, 10% glycerol, 2% $\beta$-mercaptoethanol) and size separated using 10%–15% SDS-PAGE gels, as indicated in the online Supplemental Information.

### EMSAs
The sequence 5′-TGCTAGGGGGATTTTCCCTCTCTCTGT-3′, corresponding to the consensus NF-$\kappa$B binding site (nucleotides −978 to −952) of the murine NOS-2 promoter (Castrillo et al., 2001a), was used and assayed as indicated in the online Supplemental Information.

### Measurement of IKK$\beta$ Activity
Cells ($10^7$) were homogenized in cytosolic buffer and centrifuged at 13,000 × $g$ for 15 min. The supernatant (1 ml) was precleared, and IKK$\beta$ was immunoprecipitated with 1 $\mu$g of anti-IKK$\beta$ (Castrillo et al., 2001b). After the immunoprecipitate was extensively washed with cytosolic buffer, the pellet was resuspended and assayed as indicated in the online Supplemental Information.

### Measurement of PI3K Activity
PI3K activity was measured in the anti-p85 Ab immunoprecipitates using in vitro phosphorylation of $PIP_2$ as previously described (Díaz-Guerra et al., 1999).

### In Vitro Translation of p110$\alpha$ and p110$\delta$ and Measurement of PI3K Activity
The vectors encoding *p110$\alpha$*, *p110$\beta$*, and *p110$\delta$* and the regulatory subunit p85$\alpha$ were kindly provided by Dr. Julian Downward (Cancer UK, London),

Dr. Bart Vanhaesebroeck (Queen Mary University, London) and Dr. Ana C. Carrera (CNB, Madrid). The *p110$\alpha$* and *p110$\delta$* were subcloned in a *PSG5* vector (Agilent Technologies) and transcribed and translated in vitro using the Megascript T7 kit for transcription (Life Technologies) and the TNT Quick Translation System (Promega) for translation and incorporating the transcribed *p85$\alpha$* in the translation reaction. The PI3K complexes were recovered after immunoprecipitation (IP) with anti-p85 Ab and the kinase activity was measured as previously described (Díaz-Guerra et al., 1999).

### Confocal Microscopy
Peritoneal macrophages (1 × $10^5$) were grown on coverslips and incubated with the indicated stimuli. After the covers were washed with PBS, the cells were fixed with paraformaldehyde (4%; pH 7.2) for 15 min at RT and washed again. The macrophages were permeabilized with cold methanol for 10 min at RT. After incubation with anti-phospho-S473Akt (1:500) overnight at 4°C, the cells were washed with PBS, followed by incubation with anti-rabbit secondary Ab (Alexa-Fluor 488, 1:500) for 2 hr at RT. Nuclei were revealed by staining with DAPI (1:3,000). Coverslips were mounted in Prolong Gold antifade reagent (Molecular Probes) and analyzed using an Espectral Leica TCS SP5 confocal microscope. Fluorescence intensity measurements were performed using Image J software (NIH).

### Transient Transfections
NIH 3T3 cells were maintained in Dulbecco's modified Eagle's medium (DMEM) containing antibiotics and 10% FCS. Before experiments were conducted, the medium was challenged to 1% FCS. Transient transfections were performed using FuGene HD transfection reagent (Roche), with a FuGene:DNA ratio of 8:2 and following the indications of the manufacturer (Roche). Transfection experiments were performed using vectors encoding *p110$\alpha$* wild-type (*p110WT*) and *p110$\alpha$* kinase deficient (*p110KD*) (Díaz-Guerra et al., 1999). Phosphorylation of Akt was analyzed using immunoblot as a marker of PI3K activity. In addition to this, a GFP-tagged-Akt pleckstrin homology domain (GFP-AktPH) vector kindly provided by Dr. O. Weiner (University of California, San Francisco) was used as a molecular sensor of PI3K activation upon transfection in NIH 3T3 cells, following a previously described protocol (Servant et al., 2000; Toettcher et al., 2011).

### Gene Silencing with siRNAs
Peritoneal macrophages were transfected with *Pik3ca*, *Pik3cb*, *Pik3cg*, *Pik3cd*, and nontargeting siRNAs (Thermo Scientific Dharmacon), using Lipofectamine 2,000 transfection reagent (Invitrogen) and following the manufacturer's instructions. After 48 hr, the medium was changed to RPMI medium 1,640 with 2% FCS, and the cells were stimulated for the indicated time periods for protein or RNA expression analysis.

### LPS-Induced D-GalN-Dependent Lethality Studies
An endotoxic shock was induced in male LXR$\alpha\beta^{+/+}$ and LXR$\alpha\beta^{-/-}$ mice ages 8–10 weeks old. The lethal injury was produced by i.p. injection of LPS (10 $\mu$g/kg) in combination with D-GalN (800 mg/kg). The DTPs (30 mg/kg) were administered i.p. in 0.5 ml solutol 1 hr prior to challenge with D-GalN/LPS. Solutol was given to the control animals. The lethality was monitored until 25 hr after the administration of LPS/D-GalN.

### 12-O-Tetradecanoylphorbol Acetate-Induced Mouse Ear Edema and Myeloperoxidase Activity Assay
A solution of 2 $\mu$g TPA dissolved in 20 $\mu$l DMSO was applied to both surfaces of the right ear of each mouse. The left ear (control) received the vehicle (DMSO). The DTPs were administered topically (500 ng per ear in 20 $\mu$l DMSO) simultaneously with the TPA application. The reference drug, indomethacin, was administered at the same doses. After 4 hr, the animals were killed by cervical dislocation and a 6 mm diameter disc from each ear was removed using a metal punch and weighed. Ear edema was calculated by subtracting the weight of the left ear (vehicle) from the right ear (treatment). Ear sections were homogenized in 750 $\mu$l of saline. After centrifugation at 10,000 × $g$ for 15 min at 4°C, MPO activity was measured in supernatants, as described before (Navarro et al., 1997). In addition to this, ear samples obtained at 30 min after DTP + TPA administration were homogenized and processed using western blot to evaluate the phosphorylation of Akt.

### In Vivo Administration of DTP and Ex Vivo Whole-Blood Assay

C57BL/6 mice were starved overnight and orally administrated 25 mg/kg of DTP1 and DTP5 prepared in 40% Solutol HS15 (BASF). After 90 min, whole blood was collected, as indicated in the online Supplemental Information.

### Bioluminescence Imaging of Myeloperoxidase Activity In Vivo

MPO activity was measured in the whole animal, as described previously (Gross et al., 2009). Briefly, BALB/c mice were pretreated with the DTP5 (30 mg/kg), and after 1 hr zymosan (10 mg/kg) was administered by i.p. injection. At the times indicated, luminol (5 mg in 200 μl; Sigma) was injected i.p. and the bioluminescence was recorded in an IVIS Lumina (Caliper Life Sciences).

### Microarray Analysis

RNA samples were labeled and hybridized in Agilent 4x44K one-color microarrays following the manufacturer's protocol and after two independent experiments. The slides were scanned and images were converted to raw signal txt files using Feature Extraction software (Agilent). Data preprocessing and normalization were performed using Codelink and Limma and Bioconductor packages (Gentleman et al., 2004). Differential expression was analyzed using the Limma paired t test (Smyth, 2005), as implemented in Pomelo II (Morrissey and Diaz-Uriarte, 2009). Gene-set-enrichment analysis was done using the FatiScan method in Babelomics v.3 (Al-Shahrour et al., 2006).

### Statistical Analysis

Unless otherwise stated, data are expressed as mean ± standard deviation (SD). To compare means between two independent samples, we used the Mann-Whitney rank sum test. The results were considered significant at $p < 0.05$. Data were analyzed using the SPSS for Windows statistical package v.21.

### SUPPLEMENTAL INFORMATION

Supplemental Information includes Supplemental Experimental Procedures and four figures and can be found with this article online at http://dx.doi.org/10.1016/j.chembiol.2014.06.005.

### AUTHOR CONTRIBUTIONS

P.G.T., M.A.P., and L.B. designed the research; P.G.T. and M.P-S. developed the study in animal models and the analysis of PI3K activity, P.G.T. and N.R. performed the study in MyD88-deficient mice, and P.G.T. and A.C. performed the study in LXR-deficient mice. D.R. analyzed the microarrays; T.M., E.A.T., A.C., and D.R. contributed new reagents/analytic tools; P.G.T., D.R., M.A.P., and L.B. analyzed the data; and P.G.T., M.A.P., and L.B. wrote the paper.

### REFERENCES

A-Gonzalez, N., Guillen, J.A., Gallardo, G., Diaz, M., de la Rosa, J.V., Hernandez, I.H., Casanova-Acebes, M., Lopez, F., Tabraue, C., Beceiro, S., et al. (2013). The nuclear receptor LXRα controls the functional specialization of splenic macrophages. Nat. Immunol. *14*, 831–839.

Akira, S., and Takeda, K. (2004). Toll-like receptor signalling. Nat. Rev. Immunol. *4*, 499–511.

Aksoy, E., Vanden Berghe, W., Detienne, S., Amraoui, Z., Fitzgerald, K.A., Haegeman, G., Goldman, M., and Willems, F. (2005). Inhibition of phosphoinositide 3-kinase enhances TRIF-dependent NF-κ B activation and IFN-β synthesis downstream of Toll-like receptor 3 and 4. Eur. J. Immunol. *35*, 2200–2209.

Aksoy, E., Taboubi, S., Torres, D., Delbauve, S., Hachani, A., Whitehead, M.A., Pearce, W.P., Berenjeno, I.M., Nock, G., Filloux, A., et al. (2012). The p110δ isoform of the kinase PI(3)K controls the subcellular compartmentalization of TLR4 signaling and protects from endotoxic shock. Nat. Immunol. *13*, 1045–1054.

Al-Shahrour, F., Minguez, P., Tárraga, J., Montaner, D., Alloza, E., Vaquerizas, J.M., Conde, L., Blaschke, C., Vera, J., and Dopazo, J. (2006). BABELOMICS: a systems biology perspective in the functional annotation of genome-scale experiments. Nucleic Acids Res. *34*, W472–W476.

Arbibe, L., Mira, J.P., Teusch, N., Kline, L., Guha, M., Mackman, N., Godowski, P.J., Ulevitch, R.J., and Knaus, U.G. (2000). Toll-like receptor 2-mediated NF-κ B activation requires a Rac1-dependent pathway. Nat. Immunol. *1*, 533–540.

Bremner, P., and Heinrich, M. (2002). Natural products as targeted modulators of the nuclear factor-kappaB pathway. J. Pharm. Pharmacol. *54*, 453–472.

Castrillo, A., and Tontonoz, P. (2004). Nuclear receptors in macrophage biology: at the crossroads of lipid metabolism and inflammation. Annu. Rev. Cell Dev. Biol. *20*, 455–480.

Castrillo, A., de Las Heras, B., Hortelano, S., Rodriguez, B., Villar, A., and Bosca, L. (2001a). Inhibition of the nuclear factor κ B (NF-κ B) pathway by tetracyclic kaurene diterpenes in macrophages. Specific effects on NF-κ B-inducing kinase activity and on the coordinate activation of ERK and p38 MAPK. J. Biol. Chem. *276*, 15854–15860.

Castrillo, A., Pennington, D.J., Otto, F., Parker, P.J., Owen, M.J., and Boscá, L. (2001b). Protein kinase Cepsilon is required for macrophage activation and defense against bacterial infection. J. Exp. Med. *194*, 1231–1242.

Castrillo, A., Joseph, S.B., Marathe, C., Mangelsdorf, D.J., and Tontonoz, P. (2003a). Liver X receptor-dependent repression of matrix metalloproteinase-9 expression in macrophages. J. Biol. Chem. *278*, 10443–10449.

Castrillo, A., Través, P.G., Martín-Sanz, P., Parkinson, S., Parker, P.J., and Boscá, L. (2003b). Potentiation of protein kinase C ζ activity by 15-deoxy-delta(12,14)-prostaglandin J(2) induces an imbalance between mitogen-activated protein kinases and NF-κ B that promotes apoptosis in macrophages. Mol. Cell. Biol. *23*, 1196–1208.

Chao, T.H., Lam, T., Vong, B.G., Través, P.G., Hortelano, S., Chowdhury, C., Bahjat, F.R., Lloyd, G.K., Moldawer, L.L., Boscá, L., et al. (2005). A new family of synthetic diterpenes that regulates cytokine synthesis by inhibiting IkappaBalpha phosphorylation. ChemBioChem *6*, 133–144.

Chaurasia, B., Mauer, J., Koch, L., Goldau, J., Kock, A.S., and Brüning, J.C. (2010). Phosphoinositide-dependent kinase 1 provides negative feedback inhibition to Toll-like receptor-mediated NF-kappaB activation in macrophages. Mol. Cell. Biol. *30*, 4354–4366.

de las Heras, B., Navarro, A., Díaz-Guerra, M.J., Bermejo, P., Castrillo, A., Boscá, L., and Villar, A. (1999). Inhibition of NOS-2 expression in macrophages through the inactivation of NF-kappaB by andalusol. Br. J. Pharmacol. *128*, 605–612.

de las Heras, B., Rodríguez, B., Boscá, L., and Villar, A.M. (2003). Terpenoids: sources, structure elucidation and therapeutic potential in inflammation. Curr. Top. Med. Chem. *3*, 171–185.

de las Heras, B., Hortelano, S., Girón, N., Bermejo, P., Rodríguez, B., and Boscá, L. (2007). Kaurane diterpenes protect against apoptosis and inhibition of phagocytosis in activated macrophages. Br. J. Pharmacol. *152*, 249–255.

Díaz-Guerra, M.J., Castrillo, A., Martín-Sanz, P., and Boscá, L. (1999). Negative regulation by phosphatidylinositol 3-kinase of inducible nitric oxide synthase expression in macrophages. J. Immunol. *162*, 6184–6190.

Franke, T.F., Yang, S.I., Chan, T.O., Datta, K., Kazlauskas, A., Morrison, D.K., Kaplan, D.R., and Tsichlis, P.N. (1995). The protein kinase encoded by the Akt proto-oncogene is a target of the PDGF-activated phosphatidylinositol 3-kinase. Cell *81*, 727–736.

Fukao, T., and Koyasu, S. (2003). PI3K and negative regulation of TLR signaling. Trends Immunol. *24*, 358–363.

Garantziotis, S., Hollingsworth, J.W., Zaas, A.K., and Schwartz, D.A. (2008). The effect of toll-like receptors and toll-like receptor genetics in human disease. Annu. Rev. Med. 59, 343–359.

Gentleman, R.C., Carey, V.J., Bates, D.M., Bolstad, B., Dettling, M., Dudoit, S., Ellis, B., Gautier, L., Ge, Y., Gentry, J., et al. (2004). Bioconductor: open software development for computational biology and bioinformatics. Genome Biol. 5, R80.

Gordon, S. (2007). The macrophage: past, present and future. Eur. J. Immunol. 37 (Suppl 1), S9–S17.

Gordon, S., and Martinez, F.O. (2010). Alternative activation of macrophages: mechanism and functions. Immunity 32, 593–604.

Gross, S., Gammon, S.T., Moss, B.L., Rauch, D., Harding, J., Heinecke, J.W., Ratner, L., and Piwnica-Worms, D. (2009). Bioluminescence imaging of myeloperoxidase activity in vivo. Nat. Med. 15, 455–461.

Guha, M., and Mackman, N. (2002). The phosphatidylinositol 3-kinase-Akt pathway limits lipopolysaccharide activation of signaling pathways and expression of inflammatory mediators in human monocytic cells. J. Biol. Chem. 277, 32124–32132.

Han, R., Rostami-Yazdi, M., Gerdes, S., and Mrowietz, U. (2012). Triptolide in the treatment of psoriasis and other immune-mediated inflammatory diseases. Br. J. Clin. Pharmacol. 74, 424–436.

Hazeki, K., Nigorikawa, K., and Hazeki, O. (2007). Role of phosphoinositide 3-kinase in innate immunity. Biol. Pharm. Bull. 30, 1617–1623.

Hortelano, S., Través, P.G., Zeini, M., Alvarez, A.M., and Boscá, L. (2003). Sustained nitric oxide delivery delays nitric oxide-dependent apoptosis in macrophages: contribution to the physiological function of activated macrophages. J. Immunol. 171, 6059–6064.

Jayasuriya, H., Herath, K.B., Ondeyka, J.G., Guan, Z., Borris, R.P., Tiwari, S., de Jong, W., Chavez, F., Moss, J., Stevenson, D.W., et al. (2005). Diterpenoid, steroid, and triterpenoid agonists of liver X receptors from diversified terrestrial plants and marine sources. J. Nat. Prod. 68, 1247–1252.

Jin, M.S., and Lee, J.O. (2008). Structures of the toll-like receptor family and its ligand complexes. Immunity 29, 182–191.

Kang, H.S., Kim, Y.H., Lee, C.S., Lee, J.J., Choi, I., and Pyun, K.H. (1996). Suppression of interleukin-1 and tumor necrosis factor-alpha production by acanthoic acid, (-)-pimara-9(11),15-dien-19-oic acid, and it antifibrotic effects in vivo. Cell. Immunol. 170, 212–221.

Katso, R., Okkenhaug, K., Ahmadi, K., White, S., Timms, J., and Waterfield, M.D. (2001). Cellular function of phosphoinositide 3-kinases: implications for development, homeostasis, and cancer. Annu. Rev. Cell Dev. Biol. 17, 615–675.

Kawai, T., and Akira, S. (2011). Toll-like receptors and their crosstalk with other innate receptors in infection and immunity. Immunity 34, 637–650.

Kim, J.A., Kim, D.K., Jin Tae, Kang, O.H., Choi, Y.A., Choi, S.C., Kim, T.H., Nah, Y.H., Choi, S.J., Kim, Y.H., et al. (2004). Acanthoic acid inhibits IL-8 production via MAPKs and NF-kappaB in a TNF-α-stimulated human intestinal epithelial cell line. Clin. Chim. Acta 342, 193–202.

Kumar, H., Kawai, T., and Akira, S. (2009). Toll-like receptors and innate immunity. Biochem. Biophys. Res. Commun. 388, 621–625.

Ling, T., Kramer, B.A., Palladino, M.A., and Theodorakis, E.A. (2000). Stereoselective synthesis of (-)-acanthoic acid. Org. Lett. 2, 2073–2076.

Ling, T., Chowdhury, C., Kramer, B.A., Vong, B.G., Palladino, M.A., and Theodorakis, E.A. (2001). Enantioselective synthesis of the antiinflammatory agent (-)-acanthoic acid. J. Org. Chem. 66, 8843–8853.

Mantovani, A., Sica, A., Sozzani, S., Allavena, P., Vecchi, A., and Locati, M. (2004). The chemokine system in diverse forms of macrophage activation and polarization. Trends Immunol. 25, 677–686.

Medina, E.A., Morris, I.R., and Berton, M.T. (2010). Phosphatidylinositol 3-kinase activation attenuates the TLR2-mediated macrophage proinflammatory cytokine response to Francisella tularensis live vaccine strain. J. Immunol. 185, 7562–7572.

Morrissey, E.R., and Diaz-Uriarte, R. (2009). Pomelo II: finding differentially expressed genes. Nucleic Acids Res. 37 (Suppl 2), W581–W586.

Nan, J.X., Jin, X.J., Lian, L.H., Cai, X.F., Jiang, Y.Z., Jin, H.R., and Lee, J.J. (2008). A diterpenoid acanthoic acid from Acanthopanax koreanum protects against D-galactosamine/lipopolysaccharide-induced fulminant hepatic failure in mice. Biol. Pharm. Bull. 31, 738–742.

Nathan, C., and Ding, A. (2010). Nonresolving inflammation. Cell 140, 871–882.

Navarro, A., de las Heras, B., and Villar, A.M. (1997). Andalusol, a diterpenoid with anti-inflammatory activity from Sideritis foetens Clemen. Z. Naturforsch., C, J. Biosci. 52, 844–849.

O'Neill, L.A., and Bowie, A.G. (2007). The family of five: TIR-domain-containing adaptors in Toll-like receptor signalling. Nat. Rev. Immunol. 7, 353–364.

Ogawa, S., Lozach, J., Benner, C., Pascual, G., Tangirala, R.K., Westin, S., Hoffmann, A., Subramaniam, S., David, M., Rosenfeld, M.G., and Glass, C.K. (2005). Molecular determinants of crosstalk between nuclear receptors and toll-like receptors. Cell 122, 707–721.

Palladino, M.A., Bahjat, F.R., Theodorakis, E.A., and Moldawer, L.L. (2003). Anti-TNF-α therapies: the next generation. Nat. Rev. Drug Discov. 2, 736–746.

Park, E.J., Zhao, Y.Z., Kim, Y.H., Lee, J.J., and Sohn, D.H. (2004). Acanthoic acid from Acanthopanax koreanum protects against liver injury induced by tert-butyl hydroperoxide or carbon tetrachloride in vitro and in vivo. Planta Med. 70, 321–327.

Pasare, C., and Medzhitov, R. (2004). Toll-like receptors: linking innate and adaptive immunity. Microbes Infect. 6, 1382–1387.

Prieto, P., Cuenca, J., Través, P.G., Fernández-Velasco, M., Martín-Sanz, P., and Boscá, L. (2010). Lipoxin A4 impairment of apoptotic signaling in macrophages: implication of the PI3K/Akt and the ERK/Nrf-2 defense pathways. Cell Death Differ. 17, 1179–1188.

Risco, A., del Fresno, C., Mambol, A., Alsina-Beauchamp, D., MacKenzie, K.F., Yang, H.T., Barber, D.F., Morcelle, C., Arthur, J.S., Ley, S.C., et al. (2012). p38γ and p38δ kinases regulate the Toll-like receptor 4 (TLR4)-induced cytokine production by controlling ERK1/2 protein kinase pathway activation. Proc. Natl. Acad. Sci. USA 109, 11200–11205.

Ruse, M., and Knaus, U.G. (2006). New players in TLR-mediated innate immunity: PI3K and small Rho GTPases. Immunol. Res. 34, 33–48.

Sarkar, S.N., Peters, K.L., Elco, C.P., Sakamoto, S., Pal, S., and Sen, G.C. (2004). Novel roles of TLR3 tyrosine phosphorylation and PI3 kinase in double-stranded RNA signaling. Nat. Struct. Mol. Biol. 11, 1060–1067.

Searl, T.J., and Silinsky, E.M. (2005). LY 294002 inhibits adenosine receptor activation by a mechanism independent of effects on PI-3 kinase or casein kinase II. Purinergic Signal. 1, 389–394.

Servant, G., Weiner, O.D., Herzmark, P., Balla, T., Sedat, J.W., and Bourne, H.R. (2000). Polarization of chemoattractant receptor signaling during neutrophil chemotaxis. Science 287, 1037–1040.

Smyth, G.K. (2005). Limma: linear models for microarray data. In Bioinformatics and Computational Biology Solutions using R and Bioconductor, R. Gentleman, V. Carey, S. Dudoit, R. Irizarry, and W. Huber, eds. (New York: Springer), pp. 397–420.

Tegnér, J., Nilsson, R., Bajic, V.B., Björkegren, J., and Ravasi, T. (2006). Systems biology of innate immunity. Cell. Immunol. 244, 105–109.

Toettcher, J.E., Gong, D., Lim, W.A., and Weiner, O.D. (2011). Light-based feedback for controlling intracellular signaling dynamics. Nat. Methods 8, 837–839.

Traves, P.G., Hortelano, S., Zeini, M., Chao, T.H., Lam, T., Neuteboom, S.T., Theodorakis, E.A., Palladino, M.A., Castrillo, A., and Bosca, L. (2007). Selective activation of liver X receptors by acanthoic acid-related diterpenes. Mol. Pharmacol. 71, 1545–1553.

Trinchieri, G., and Sher, A. (2007). Cooperation of Toll-like receptor signals in innate immune defence. Nat. Rev. Immunol. 7, 179–190.

Troutman, T.D., Bazan, J.F., and Pasare, C. (2012). Toll-like receptors, signaling adapters and regulation of the pro-inflammatory response by PI3K. Cell Cycle 11, 3559–3567.

van Dop, W.A., Marengo, S., te Velde, A.A., Ciraolo, E., Franco, I., ten Kate, F.J., Boeckxstaens, G.E., Hardwick, J.C., Hommes, D.W., Hirsch, E., and van den Brink, G.R. (2010). The absence of functional PI3Kγ prevents leukocyte recruitment and ameliorates DSS-induced colitis in mice. Immunol. Lett. 131, 33–39.